ELSEVIER

Biochimica et Biophysica Acta 1238 (1995) 183–191

BBA Biochimica et Biophysica Acta

Charge determination of membrane molecules in polymer-supported lipid layers

Christian Dietrich [a], Robert Tampé [a,b,*]

[a] *Lehrstuhl für Biophysik E22, Physik Department, Technische Universität München, D-85478 Garching, Germany*
[b] *Max-Planck-Institut für Biochemie, Am Klopferspitz 18a, D-82152 Martinsried, Germany*

Received 29 March 1995; accepted 16 May 1995

Abstract

A method for two-dimensional micro-electrophoresis and charge determination of fluorescence-labeled membrane molecules in lipid layers is presented. Therefore, the labeled molecules are dissolved in a lipid monolayer which acts as a fluid matrix. The essential part of the sample preparation is an aqueous polymer film composed of agarose onto which the layer is transferred by Langmuir-Blodgett technique. The induced force of an applied electric field leads to a drift of the charged fluorescent molecules. The mobility is determined by an analysis of the steady-state bleach profile which is produced by continuous fluorescence micro-photolysis of a rectangular area of the monolayer. Testing a variety of amphiphilic molecules, measurements yielded values of zero, plus or minus one elementary net charge within a margin of error. The experimental set-up described here can be used for lateral separation, enrichment and isoelectric focusing of membrane components.

Keywords: Lipid monolayer; Polymer; Membrane; Electrophoresis; Photobleaching; FRAP; Diffusion

1. Introduction

Many investigations of organic films deposited on solid surfaces, such as nanofabricated silicon, glass or thin metal(oxide) films have been carried out. Although polymers have different and intriguing qualities in comparison to solids, there have been only few attempts to use polymers as substrates for thin organic films so far. We have previously demonstrated that polymeric gels composed of polyacrylamides defined by the monomer concentration and cross-linking ratio are promising for lipid monolayers and bilayers [1]. Here, a homogeneous fluid lipid membrane is deposited on an aqueous polymer of agarose, which provides some important advantages for micro-electrophoresis and charge determination of membrane components in lipid membranes.

The analysis of the electrophoresis phenomenon in small dimensions, where surface-to-volume ratio plays a key role, such in capillary electrophoresis, showed that the velocity of the drifting molecule is mainly determined by two processes: (i) the direct force of the electric field on charged molecules (electrophoresis); (ii) the induced flow of mobile counter ions coupling to the lipid layer (electroosmosis). On glass-supported bilayers, where the drift of charged lipids in an applied electric field has been analyzed by pattern photobleaching [2] the two effects overlapped: the electroosmosis was difficult to control and was therefore the main restriction of electrophoresis and charge determination of membrane molecules in lipid membranes, especially for larger molecules. To avoid this problem, a composite polymer-membrane system was generated, which in addition opens up the possibility to reconstitute and electrophoretically separate even larger molecules such as integral membrane or lipid anchored proteins. The advantages of polymeric fluids in interfaces to reduce the electroosmotic effect have already been successfully applied in capillary electrophoresis [3].

Amphipathic molecules varying in their net charge are used as model compounds and traced with fluorescent dyes. The separation and drift velocity of these fluorescent molecules which are homogeneously dissolved in the polymer-supported, fluid membrane matrix was determined by

* Corresponding author. E-mail: tampe@vms.biochem.mpg.de. Fax: +49 89 85782641.

SSDI 0005-2736(95)00129-8

the analysis of the bleach profiles of continuous illumination experiments. During continuous illumination of a limited area the change of fluorescence intensity is determined by the bleach process and by the flux of intact dyes into the detection area. When these two effects compensate each other, a steady-state situation is reached, and the fluorescence intensity remains constant. A related technique has been previously used to determine diffusion constants by analysis of time-dependent fluorescence decay [4,5]. In experiments described herein, a concentration profile is recorded after approaching steady-state, in order to determine the net-charge of fluorescent membrane components. No time resolution is required, and therefore averaging processes can be applied to improve the signal-to-noise ratio. Furthermore, disturbances during the experiment are less critical as the system always approaches steady-state. For that reason, this continuous photobleach method is a practical alternative to other well established techniques using short bleach pulses prior analysis of the fluorescence recovery, e.g., fluorescence recovery after photobleaching (FRAP) [6], total internal reflection – FRAP [7] or pattern photobleaching [2]. Combining the advantages of steady-state bleaching with the polymer-supported lipid layers, we are able to dissect the electrophoresis process and perform charge determination of membrane molecules in their natural environment.

2. Materials and methods

2.1. Experimental set-up of the micro-electrophoresis

The experimental set-up and a schematical view of the two-dimensional micro-electrophoresis in lipid layers is illustrated in Fig. 1. As a substrate for the Langmuir-Blodgett deposition we used a glass slide equipped with electrodes connected to a high voltage supply. The slide was coated with an agarose film of approx. 0.5 μm thickness onto which a lipid monolayer was transferred. In order to reach 100% humidity needed for the experiments, the coated glass slide with the lipid monolayer face down is laid on top of a tempered Teflon chamber (PTFE) partially filled with water. For temperature control, peltier elements were placed below the base-plate (accuracy $\pm$ 0.2°C). All experiments were performed at 25°C. This set-up is placed under an epi-fluorescence microscope which was described previously [8]. The lipid deposition is controlled by comparison of the fluorescence picture before and after lipid transfer onto the substrate. A HBO 50 mercury lamp (Osram, Germany) aligned for Köhler illumination served as light source. For the continuous bleach experiments the round field diaphragm was replaced by a slit. The use of a long working distance objective allows the correction for glass slides up to a thickness of 2 mm (CDPlan 40, aperture 0.6; Olympus, Japan). Two easily interchangeable filter systems (Zeiss, Germany) adapted for fluorescence dyes with excitation wavelengths at 480 nm or 560 nm and emission wavelengths at 550 nm or 620 nm, respectively, are used. Fluorescence micrographs are recorded by a SIT-camera (C 2400, Hamamatsu) and analyzed by a commercial image processing system on a Macintosh computer providing to a spatial resolution of 0.405 μm^2 per pixel. The intensity is transformed into integer gray values from 0 to 255. Control experiments with gray filters demonstrate a linear relationship between fluorescence intensity and gray values of the image processing system. An improvement of the signal-to-noise ratio is achieved by temporal and spatial averaging processes.

2.2. Preparation of the polymer substrates

As a support for the polymeric gel a well cleaned glass slide (38 × 25 × 1 mm) is used. Chrome electrodes (0.5 μm thick) are evaporated onto the glass slide. Coating with agarose is performed by dipping the glass slide into an agarose-water solution (0.2% w/w agarose) at a temperature above the gelation point of the agarose. The polymer solution is buffered with 10 mM Hepes, pH 7.0. When the glass is pulled quickly out of the solution, a thin film of the polymer solution remains on the glass [9], as measured by means of reflection interference contrast microscopy [10,11]. The thickness of the dry polymer was determined to be in the range of 0.5 μm. Agarose is purchased in IEF-quality (Sigma, Germany).

2.3. Lipid monolayer deposition

As an uncharged matrix lipid for the electrophoresis experiments, L-α-dimyristoylphosphatidylcholine (DMPC) is used (Avanti Polar-Lipids, USA). *N*-(7-Nitrobenz-2-oxa-1,3-diazol-4-yl)dimyristoylphosphatidylethanolamine (NBD-DPPE), 1,1′-dioctadecyl-3,3,3′,3′-tetramethylindocarbocyanine perchlorate (D282) and 4-(*N*,*N*-dihexadecyl)amino-7-nitrobenz-2-oxa-1,3-diazole (D69) are purchased from Molecular Probes (Eugene, USA). All molecules are dissolved in chloroform (HPLC quality). These fluorophores are mixed with the matrix lipid in the molar ratio of 98:2 (lipid/dye). To avoid lateral stress induced by temperature gradients, all depositions (Langmuir-Blodgett technique) are performed at 25°C. Transfers of the monolayers (3 Å^2/molecules per min) are carried out at a lateral pressure of 20 mN/m which is kept constant by an electronic feedback control of the film area. The surface tension was measured with a Wilhelmy system (accuracy $\pm$ 0.1 mN/m).

2.4. Numerical simulation of the photobleach process

In order to have an additional approach to the continuous bleach processes, numerical simulations are performed. Analogously to the experimental set-up, the simu-

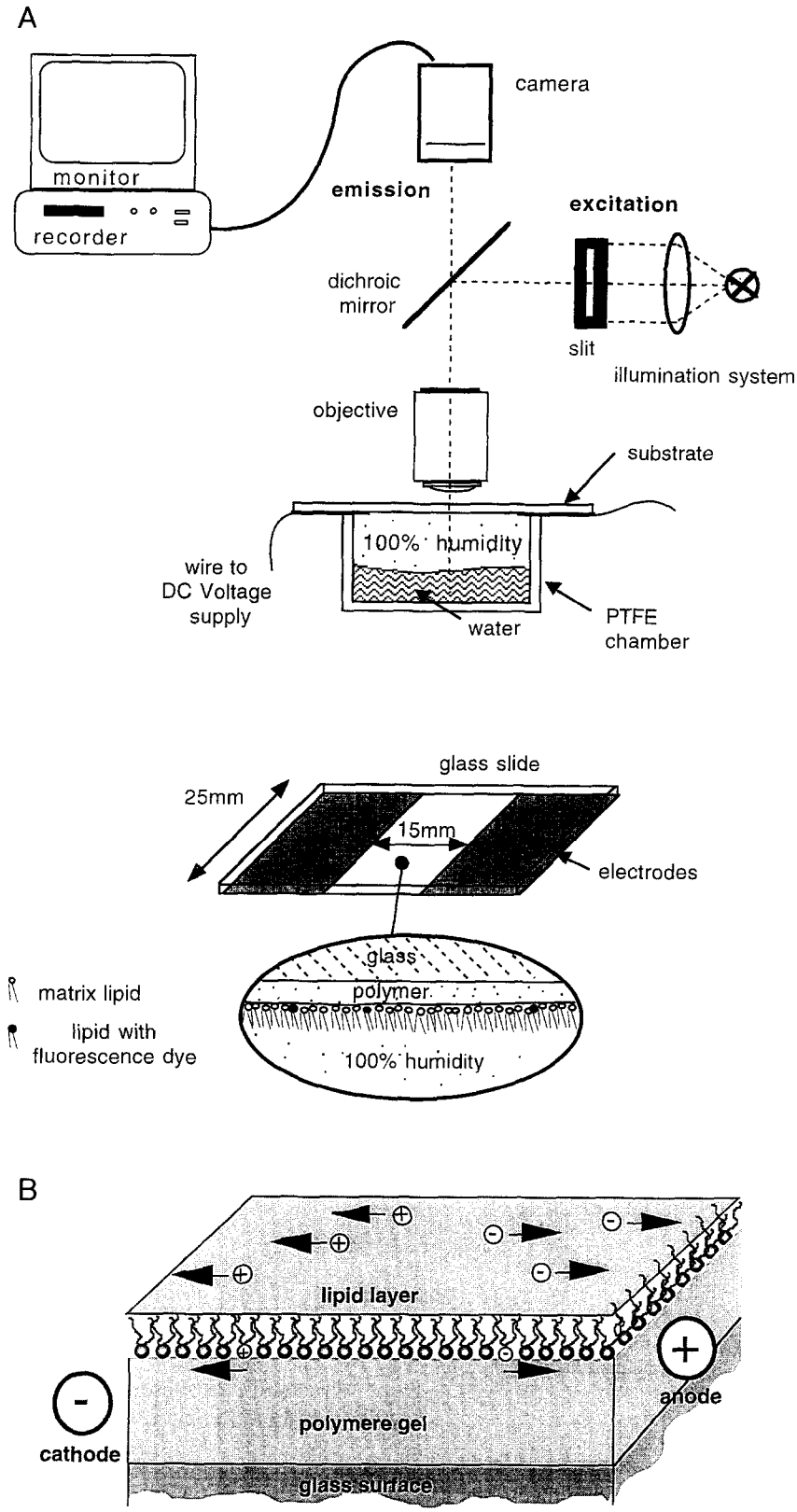

Fig. 1. (A) The central part of the set-up is an epi-fluorescence microscope. The prepared monolayer is placed below the microscope so that the border lines of the chrome electrodes and the illuminated slit are parallel. The applied electric field induces a drift of the charged molecules perpendicular to this orientation. (B) Schematical view of the micro electrophoresis in polymer-supported lipid monolayers.

lation starts at constant fluorophore concentration (c_0). The temporal development of the dye intensity is gained by numerical evaluation of the differential equation Eq. (4). Therefore, the Runge-Kutta algorithm of fourth order is used [12]. The step size between two evaluated profiles corresponds to a time interval of 0.1 s. The resolution of the simulated profiles was 1 point/μm. The size of the simulated region is enlarged until the bleach process in the slit region has no influence on the concentration at the borders of the simulated profile anymore. Numerically simulated and measured intensity profiles are analyzed by χ^2-fitting following Levenberg and Marquardt [12]. For measured profiles, the fits are weighted with the standard deviation of each point.

2.5. Steady-state photobleach experiments

For charge determination, an electrophoresis experiment is performed in the following way: the coated glass slide is oriented under the microscope with the electrodes parallel to the edges of the illuminated slit region. The used slits are in the range of 60–80 μm wide. The intensity profile is determined within a distance of 162 μm, perpendicular to the slit. The time required to approach steady-state depends on the experimental conditions. In practice the bleach period is 10–60 min. The slit is removed after reaching steady-state (constant fluorescence intensity). Examples of the bleach profile in the absence and presence of an external electric field are given in Fig. 3. To reduce noise a temporal and spatial averaging is carried out.

For the evaluation of the diffusion constant, a separate determination of the bleach constant is necessary. Therefore, a round area of the monolayer with 150 μm in diameter is illuminated and the decay of fluorescence intensity is detected in its center as follows: in intervals the video signal is averaged for 0.33 s (8 video pictures) to produce a time-averaged image. 1600 central pixels (square area of 16×16 μm $= 40 \times 40$ pixels) of this image are used to perform a second averaging. The mean value obtained is one point of the intensity trace which is fitted by an exponential function. The exponent equals the bleach constant. The gray value of zero intensity is a further parameter in the fitting procedure of the time trace.

3. Results

3.1. Theory and simulation of continuous photobleach experiments

Considering the intensity profile of a fluorescence dye, which is induced by a continuous bleach process in a restricted region, $c(\vec{x},t)$ is the concentration of the dye at x and t. The time-dependence of the concentration is described by to two processes.

First, the bleaching of dyes which ideally follows a first order process:

$$\left.\frac{\partial c}{\partial t}\right)_{\text{bleach}} = -Ic(\vec{x},t) \tag{1}$$

where I is the bleach constant determined by the properties of the dye itself and by the intensity of the illumination.

Second, the flux of dye which is induced by a concentration gradient or an external field:

$$\left.\frac{\partial c}{\partial t}\right)_{\text{flux}} = -\text{div}(\vec{j}) = -\text{div}(-D \cdot \text{grad}(c) + c\vec{v}_{\text{drift}}) \tag{2}$$

where D is the diffusion constant, $\vec{v}_{\text{drift}}$ is the average drift velocity of dyes, and $\vec{j}$ corresponds to the flux of dyes. If steady-state is reached, c_{ss} fulfills the following equation:

$$\frac{\partial c_{ss}}{\partial t} = 0 = \left.\frac{\partial c_{ss}}{\partial t}\right)_{\text{bleach}} + \left.\frac{\partial c_{ss}}{\partial t}\right)_{\text{flux}} \tag{3}$$

The length of the slit (y) is much larger than its width (x). As the concentration in the y-direction is considered constant, the geometry is reduced to one dimension.

In the case of a drift in x-direction, the steady-state profile is given by the differential equation:

$$0 = D\frac{\partial^2 c_{ss}}{\partial x^2} - v_{\text{drift}}\frac{\partial c_{ss}}{\partial x} - Ic_{ss} \tag{4}$$

with

$I = I_0$ for $x_{lb} < x < x_{rb}$ (slit region)

$I = 0$ for $x > x_{rb}$, $x < x_{lb}$ (outside)

In the case of $v_{\text{drift}} > 0$ the solution for the equation is:

$$c_{ss} = \beta_1 - \beta_2\exp(2\tilde{q}x) \quad \text{for } x < x_{lb} \tag{5}$$

$$c_{ss} = \beta_3\exp(\tilde{q}x)[\exp(-bx) + \beta_4\exp(bx)]$$

$$\approx \beta_3\exp((\tilde{q} - b)\cdot x) \quad \text{for } x_{lb} < x < x_{rb} \tag{6}$$

$$c_{ss} = \beta_5 \quad \text{for } x > x_{rb} \tag{7}$$

with

$$\tilde{q} = \frac{v_{\text{drift}}}{2D} \qquad b = \sqrt{\left(\frac{v_{\text{drift}}}{2D}\right)^2 + \frac{I_0}{D}}$$

The coefficients are determined by the border conditions of the differential equation:

$$\beta_1 = c_0$$

$$\beta_2 = (\beta_1 - \beta_3(\exp((\tilde{q} - b)x_{lb}) + \beta_4\exp((\tilde{q} + b)x_{lb})))$$

$$\times\exp(-2\tilde{q}x_{lb})$$

$$\beta_3 = \beta_1 \left[\begin{array}{l} \exp((\tilde{q}-b)x_{rb})\left(1+\dfrac{I_0}{v_{drift}(\tilde{q}-b)}\right) \\ -\exp((\tilde{q}-b)x_{lb})\left(\dfrac{I_0}{v_{drift}(\tilde{q}-b)}\right) + \\ \beta_4\left\{\exp((\tilde{q}+b)x_{rb})\left(1+\dfrac{I_0}{v_{drift}(\tilde{q}+b)}\right)\right. \\ \left. -\exp((\tilde{q}+b)x_{lb})\left(\dfrac{I_0}{v_{drift}(\tilde{q}+b)}\right)\right\} \end{array} \right]^{-1}$$

$$\beta_4 = \frac{b-\tilde{q}}{b+\tilde{q}}\exp(-2\,b\,x_{rb})$$

$$\beta_5 = \beta_3(\exp((\tilde{q}-b)x_{rb}) + \beta_4\exp((\tilde{q}+b)x_{rb}))$$

$v_{drift} < 0$ can be transferred to $v_{drift} > 0$ by a reflection of the x-axis. Further discussions relate to $v_{drift} > 0$.

The fluorophore concentration of the analytic steady-state solution is limited for $x \to \pm\infty$ which corresponds to the experimental situation. In the slit region $x_{lb} < x < x_{rb}$, an approximation for the concentration profile at steady-state can be given by a simple exponential function with an exponent $(\tilde{q}-b)$ (Eq. (6)). The second term $\beta_4\exp(bx)$ of the accurate solution can be neglected since it approaches the first term $\exp(-bx)$ only at the right border of the slit. The first term which exponentially decreases with increasing x has its smallest value at this point.

The steady-state profile is evaluated by using Eqs. (5)–(7) and presented as a solid line in Fig. 2A. The dashed curves reflect the numerical simulation of the bleach experiment. The parameters are identical for all traces and given in the legend. The initial situation is in agreement with experimental conditions at a constant dye concentration $C(x,t=0) = C_0$. Fitting the region $x < x_{lb}$ of the simulated profiles with the analytic solutions of Eq. (5) provides a value for $2\tilde{q} = v_{drift}/D$. In the slit region $(x_{lb} < x < x_{rb})$, fits are carried out by the approximated analytic solution given in Eq. (6). Here, the fitted exponent is divided by the term

$$(\tilde{q}-b) = \frac{v_{drift}}{2D} - \sqrt{\left(\frac{v_{drift}}{2D}\right)^2 + \frac{I_0}{D}}$$

which is evaluated by the chosen parameters.

In Fig. 2B, the ratios between the fitted values and the exponents used to evaluate the analytic steady-state curve are displayed for $x < x_{lb}$ (open circles) and $x_{lb} < x < x_{rb}$ (closed circles). After 8 min, the deviation is less than 5%. After 15 min, hardly any deviation from the steady-state curve is detectable. This is correlated with a constant fluorescence intensity in the slit region (asterisks).

In our case, the drift is induced by an electric field acting on the charged membrane molecules. For weak

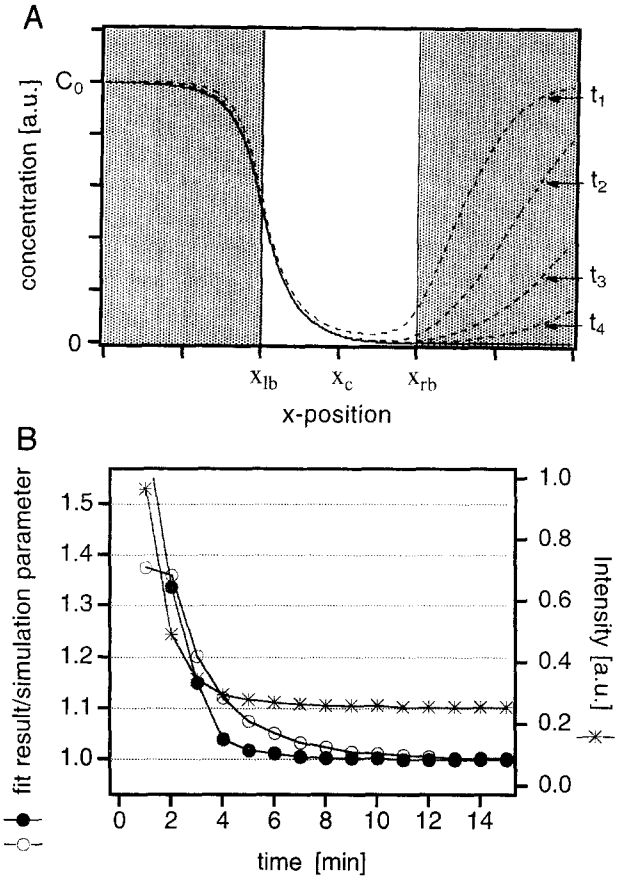

Fig. 2. The solution at steady-state is compared with intensity profiles evaluated by a numerical simulation of the bleach process. The physical parameters have the following values: diffusion constant 3 $\mu m^2/s$, slit width 100 μm, bleach constant in the slit is 0.02 s^{-1} (no illumination beside the slit), drift velocity is $v_{drift} = 0.2\ \mu m/s > 0$. (A) The dashed lines are profiles generated by a numerical simulation of the continuous bleach experiment. Corresponding to the experimental set-up, simulations start with a constant dye concentration c_0. The traces show profiles which were created after bleach periods of 3, 6, 10 and 15 min indicated with t_1, t_2, t_3, t_4. The trace at steady-state (solid line) was evaluated with Eqs. (5)–(7). This curve fulfills the border condition of a limited dye concentration with $\lim_{x \to -\infty} c(x,t) = c_0(=\beta_1)$. (B) In the region left to the slit $(x < x_{lb})$, the simulated profiles were fitted with the analytic function described in Eq. (5). The fitted exponents for v_{drift}/D were divided by the exponent used to evaluate the equilibrium trace of Fig. 2A. The quotients are traced by open circles. In the slit region $(x_{lb} < x < x_{rb})$ the profiles were fitted by the approximated analytic solution (see Eq. (6)). The fitted exponents for $(\tilde{q}-b)$ were divided by the corresponding value $\frac{v_{drift}}{2D} - \sqrt{\left(\frac{v_{drift}}{2D}\right)^2 + \frac{I_0}{D}}$. The quotients are traced by closed circles. Asterisks illustrate the fluorescence intensity integrated in the slit region of the simulated profiles.

forces a linear relationship between field and induced drift velocity can be assumed:

$$v_{drift} = \mu q E \qquad (8)$$

with μ = mobility, q = charge, and E = electric field.

Using the Einstein relationship $D = \mu kT$, the charge q

of the molecule is proportional to the quotient of drift velocity and diffusion constant:

$$q = \left(\frac{v_{drift}}{D}\right)\frac{kT}{E} = \tilde{q}\frac{2kT}{E} \quad (9)$$

$$E = U/d \quad (10)$$

The electric field E is given by the applied voltage U and the distance d between the electrodes. k is the Boltzmann factor and T is the temperature in degrees Kelvin.

In consequence, the exponent of the steady-state curve on the left side of the slit $v_{drift} > 0$ is directly proportional to the charge of the drifting molecule (Eqs. (5) and (9)). Due to this simple relationship, the charge of various membrane components can be easily determined by analysis of the steady-state fluorescence profile as shown in the next section.

3.2. Micro electrophoresis in polymer-supported membranes

In Fig. 3 bleach profiles of a DMPC/NBD-DPPE (molar ratio 98:2) monolayer supported on an agarose gel in the absence (Fig. 3A) and presence (Fig. 3B) of an external electric field (E = 10 V/cm) are illustrated. The anode is on the left side. After continuous photobleaching, the slit is removed and pictures are taken as described. The negatively charged dyes drift from the right side into the illuminated region where a part of the dyes is bleached. This leads to a decrease of fluorescence on the left side. The gray values of each bleach profile are shown at the bottom of Fig. 3. The transition from bleach profile in Fig. 3A to that in Fig. 3B is comparable to a second-order phase transition, whereby the drift induced by the external

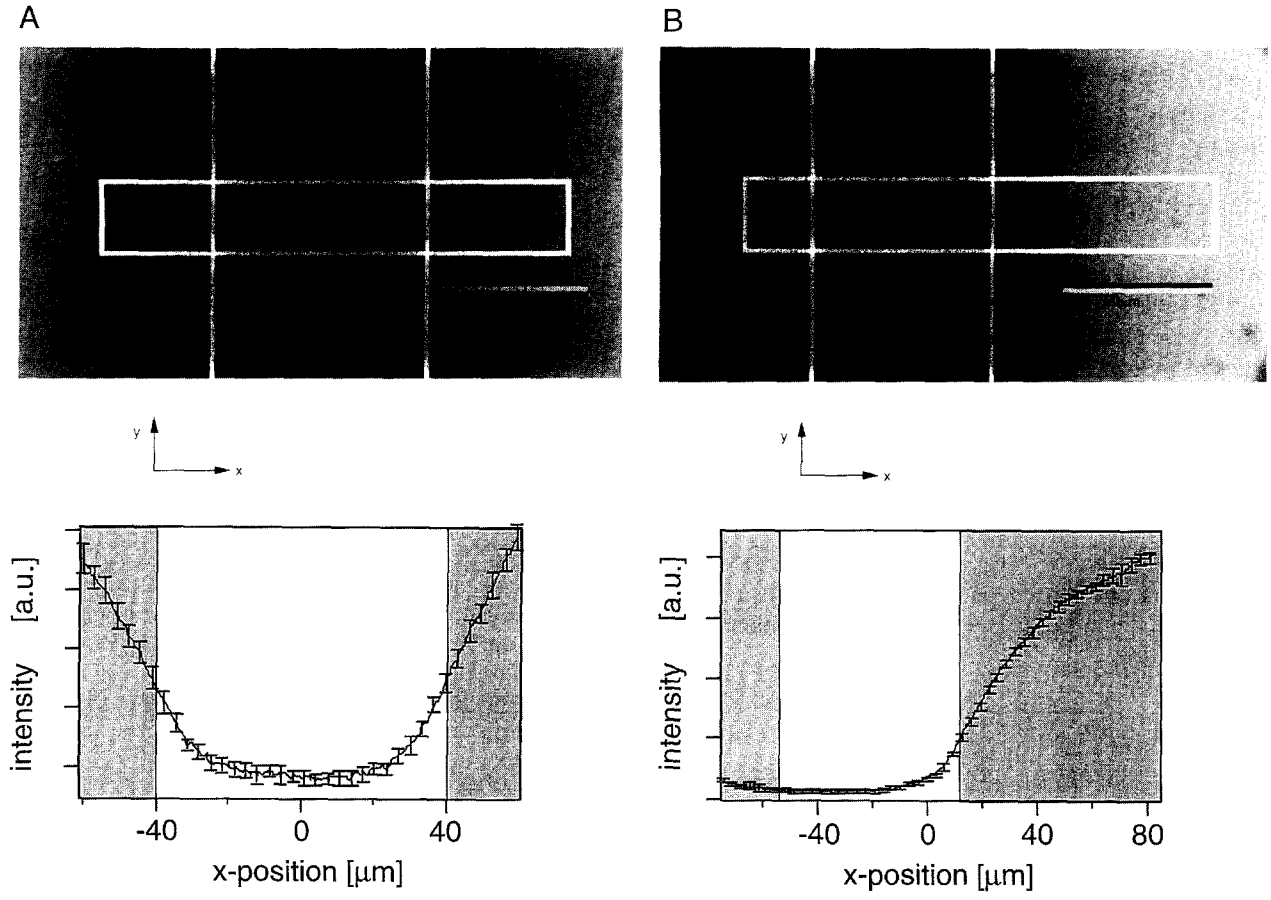

Fig. 3. Bleach profiles of a DMPC/NBD-DPPE monolayer (molar ratio 98:2) are shown which are deposited on an agarose substrate at 20 mN/m (25°C). Images were taken after the slit was removed. The images were obtained by time averaging of 24 frames (1 s). In the center the bright frame with dimension ($x \times y$) of 400 × 60 pixels (162 × 23 μm) indicates the area used for analysis of the profile. The 60 pixels at the same x-position were averaged. The profiles are shown in the bottom panels. For every eighth point of the traces the standard deviation of the spatial averaging is indicated by error bars. (A) Without an electric field the intensity profile (after a bleach period of 11 min) is symmetric. (B) In the presence of an electric field (10 V/cm, anode is on the left side) the symmetry disappears (bleach period 40 min).

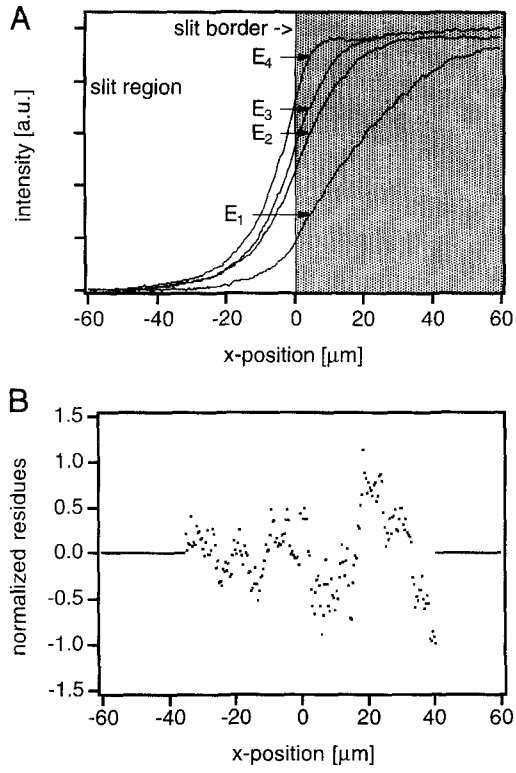

Fig. 4. (A) Steady-state bleach profiles of a DMPC/NBD-DPPE (98:2) monolayer at different electric field strengths (E_{1-4} = 10.0, 20.0, 26.7, 53.3 V/cm). The anode is on the left side. For comparison the profiles are normalized ($c_0 = 1$). (B) As a representative example ($E_2 = 20$ V/cm), the normalized residue (the deviation of measurement and fit normalized by the standard deviation of each measured data point) demonstrates the quality of the performed fit. The fit right beside the slit is performed with Eq. (5) (here $\nu_{drift} < 0$). The slit region is fitted with the approximation described in Eq. (6). The residues are smaller than 1, but the deviations are not statistically distributed. This reflects the fact that the intensity of neighbored points are correlated. In regions where no fit was carried out the residue is set to zero.

field leads to a loss of the reflection symmetry resulting in completely different profiles. In the case of this additional drift, only one curve fulfills the steady-state equation for a given set of physical parameters. This leads to a constant fluorescence intensity after approaching equilibrium.

All experiments described were performed with DMPC monolayers deposited on agarose gels. Three different fluorescence labeled lipids were analyzed: the positively charged D282 ($+e$), the uncharged D69 and the negatively charged NBD-DPPE ($-e$). For all voltages applied no current was detected (< 2 μA). In Fig. 4A, the steady-state profiles of NBD-DPPE are displayed for different electrical fields (E_{1-4} = 10.0, 20.0, 26.7, 53.3 V/cm) with the anode is at the left side ($\nu_{drift} < 0$). In the experiments with NBD-DPPE and D282, bleach periods take up to 40 min. For the neutral dye D69, where hardly any drift could be induced, a bleach period of nearly 1 h is necessary to approach steady-state.

The quality of an applied fit is shown in Fig. 4B for $E_2 = 20$ V/cm as an example. The quotient ν_{drift}/D is determined by the fit right/left beside the slit ($\nu_{drift} < 0/\nu_{drift} > 0$). As Eq. (5) indicates, the intensity follows exponential behavior. The slit region is fitted with the approximation of the analytic solution (Eq. (6)). Unlike the analysis of the simulated profiles, fit functions contain one further fit parameter representing the intensity of the off-set. Since the weighted residue is smaller than 1, the deviation is significantly smaller than the standard deviation of the values.

The analysis of all measured drift profiles is summarized in Fig. 5A. The charge of the molecules is given by the slope of the fitted curve (Eq. (9)). For the uncharged molecule D69, only a very small, but significant drift can be detected which corresponds to a charge of $0.03e$ ($\pm 25\%$). For NBD-DPPE or D282, a net-charge of $-0.97e$

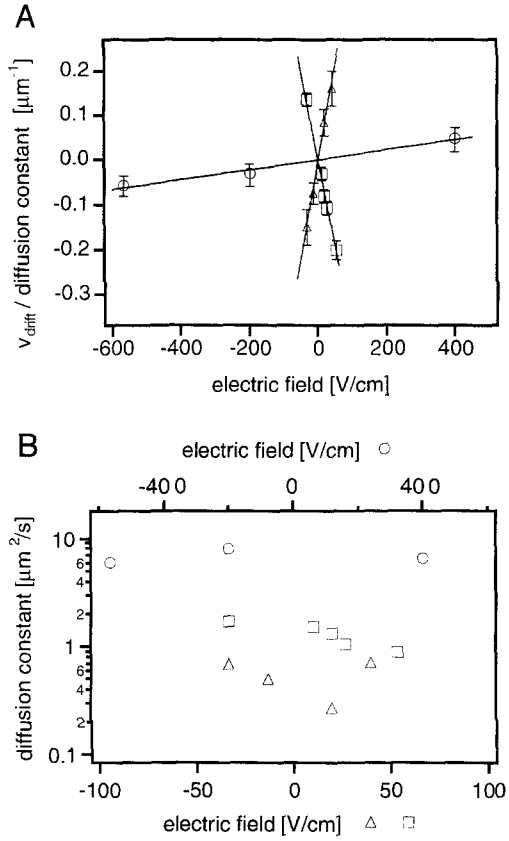

Fig. 5. Two-dimensional electrophoresis experiments of various dye molecules incorporated in a polymer-supported DMPC monolayer. The results of the charge determination (A) and diffusion constant (B) of the dyes NBD-DPPE (rectangles), D69 (circles), and D282 (triangles) are illustrated. The measurements provide the quotient ν_{drift}/D as a function of different electric fields. The error was determined by variation of the fit parameters up to the point were a drastic increase in χ^2 occurs. The slope of the fitted lines is proportional to the charge of the dye molecule (Eq. (9)). In order to control if the measured charges lead to consistent diffusion coefficient D is determined by two additional fits (see text). The error is the sum of the uncertainties of the bleach constant and the fits of the different regions. Since the obtained data serve only as a control, they are shown without any error bar.

Probes in agarose-supported DMPC monolayer	NBD-DPPE	D69	D282
	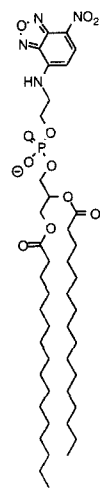	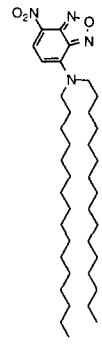	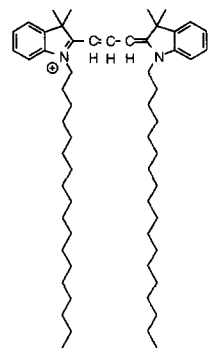
charge	- e	0	+ e
charge measurement	- 0.97 e (± 14 %)	+ 0.03 e (± 25 %)	1.08 e (± 14 %)
diffusion constant (± 40%)	2 $\mu m^2/s$	9 $\mu m^2/s$	0.5 $\mu m^2/s$
bleach constant (± 20%)	0.029 s^{-1}	0.0034 s^{-1}	0.00078 s^{-1}

Fig. 6. A summary of structure, charge, diffusion and bleach constant of lipid probes is given by using DMPC as uncharged matrix lipid. The monolayer were transferred on agarose at 20 mN/m and 25°C. The ratio matrix lipid/fluorescence dye was always 98:2.

and $+1.08e$ is measured, respectively. The deviation from the elementary charge ($\pm e$) is in the range of error ($\pm$ 14%). As a cross-check if the fitted charge values lead to a consistent measurement of the diffusion constant, a further analysis of the slit region is performed. In combination with the determined quotient v_{drift}/D and the bleach constant I_0, the fitted value of the exponent $(\tilde{q} - b)$ allows the evaluation of the diffusion constant. The results are shown in Fig. 5B (open markers). Here, the error of the determined values is evident, since three terms have to be determined separately. Though the diffusion coefficients of the labeled lipids are consistent for each dye, the values vary from 0.5 $\mu m^2/s$ (D282) to 9 $\mu m^2/s$ (D69). The difference between diffusion constants of different dyes reflects their individual molecular geometry. The diffusion coefficients are in good agreement to data obtained by FRAP measurements performed on the same monolayer (data not shown). The results of the charge measurements, diffusion and bleach constant are summarized in Fig. 6.

4. Discussion

In this article, we describe the charge determination of fluorescent membrane molecules embedded in polymer-supported lipid monolayers. These novel polymer supports have interesting aspects and combine some effective advantages: at high humidity only weak coupling of the lipids to the polymer occurs which maintains the fluidity and leads to a nearly undisturbed monolayer. In comparison to glass supports, the diffusion constant is increased by a factor of about 30 and the fluorescence is more homogeneous. In contrast to a self-organized lipid monolayer at the air-water interface, the polymer support suppresses convection effects. Recently, we have characterized polymer-supported monolayer and bilayer in detail, including studies on the frictional coupling between lipid monolayer and the polymer, polymer heterogeneity, the hydration, and the lipid layer stability [1].

Despite the lipid layer being decoupled from the solid surface, the following points demonstrate that there is still a weak interaction with the polymeric network: (i) In comparison to a 'free' lipid monolayer at the air-water interface [5], the diffusion constant is smaller by a factor of about 10 (see Fig. 6). (ii) In case of polymer-supported bilayers the diffusion of lipopeptides protruding into the polymeric network (proximal layer) is hindered in comparison to the lipopeptides in the distant layer [1].

In case of micro-electrophoresis experiments and charge determination of membrane components in lipid layers, the reduction of electroosmosis at the fluid lipid interface is crucial. Though there is still a detectable drift of an

uncharged molecule, a drastic decrease of electroosmosis can be achieved (Fig. 5A, Fig. 6) in comparison to electrophoresis measurements in glass-supported bilayers [2]. This effect makes the polymer support a prerequisite for the performance of charge determination, even for larger molecules. The charge determination is performed by a continuous bleach method. During electrophoresis and continuous illumination of a limited area, the fluorescence profile approaches a steady-state situation which is determined by the bleach process, diffusion and drift of intact dyes. In comparison to other photobleach techniques this method has some effective advantages in comparison to other photobleach techniques: (i) we are looking at an equilibrium situation. This means that no time resolution is required which can be utilized to optimize the signal-to-noise ratio. Consequently, the method is less sensitive to disturbances. (ii) The variability of illumination intensity (gray filter) enables adaptation to physical parameters. (iii) A simple experimental set-up including an epi-fluorescence microscope is necessary. (iv) In the case of charge measurements the quotient v_{drift}/D is directly determined and a separate analysis of each parameter is not necessary. The determined values correspond to the expected values in the range of error. In comparison, the following disadvantages of the continuous bleach method must be taken into account: (i) the steady-state situation is approached but never really reached. If the experimental parameters are poorly chosen, the resulting profile will differ from the steady-state profile remarkably even after long bleach periods. (ii) To determine the diffusion constant a separate analysis of the bleach constant and the quotient $1/D$ is necessary. This leads to a sum of errors.

Gel-supported membranes have new interesting aspects. In analogy to nature the polymer network of agarose is bioadaptable per se and due to the weak coupling it holds the lipid layer in an undisturbed state on the solid support. In this work we focused on one special application of polymer supports as crucial preparation for micro-electrophoresis and charge determination of membrane molecules. The separation of the lipid layer from solid supports by a soft polymer cushion opens new possibilities for the preparation of bioadaptable substrates and 'phantom cells' studying cell-cell recognition and membrane translocation processes. In addition, these polymers can be functionalized (e.g., by substrates and reactive groups) and structured in two dimensions. This opens the field for various applications. Preparing a pH-gradient in the gel a two-dimensional micro isoelectric focusing of various membrane molecules might be possible. Membrane components could be separated and analyzed by means of sensitive optical techniques and electrical measurements. These molecules could be enriched and patterned in arrays.

Acknowledgements

We thank Martin Kühner for carrying out the FRAP measurements and Dr. Erich Sackmann for continuous encouragement. This work was supported by the Bundesminister für Forschung und Technologie.

References

[1] Kühner, M., Tampé, R. and Sackmann, E. (1994) Biophys. J. 67, 217–226.
[2] Stelzle, M., Mielich, R. and Sackmann, E. (1992) Biophys. J. 63, 1346–1354.
[3] Mazzeo, J.R., Martineau, J.A. and Krull, I.S. (1992) Methods: A Companion to Methods in Enzymology 4, 205–212.
[4] Peters, R., Brünger, A. and Schulten, K. (1981) Proc. Natl. Acad. Sci. USA 78, 962–966.
[5] Meller, P. (1985) Thesis, Technical University, Munich.
[6] Axelrod, D., Koppel, D.E., Schlessinger, J., Elson E.L. and Webb W.W. (1976) Biophys. J. 16, 1055–1069.
[7] Thompson, N.L., Burghardt, T.P. and Axelrod, D. (1981) Biophys. J. 33, 435–454.
[8] Dietrich, C., Schmitt, L. and Tampé, R. (1995) Proc. Natl. Acad. Sci. USA 92, in press.
[9] De Gennes P.G. (1986) Colloid Polymer Sci. 264, 463–465.
[10] Rädler, J. and Sackmann, E. (1993) J. Phys. II France 3, 727–748.
[11] Gritsch, S., Neumaier, K., Schmitt, L. and Tampé, R. (1995) Biosensors Bioelectronics, in press.
[12] Press W.H., Flannery B.P., Teukolsky S.A. and Vetterling W.T. (1989) Cambridge University Press, 2nd Edn.